Analyst

PAPER

View Article Online
View Journal | View Issue

Cite this: *Analyst*, 2014, **139**, 6259

A recyclable chitosan-based QCM biosensor for sensitive and selective detection of breast cancer cells in real time

Shaolian Zhang,[a] Haihua Bai,[a] Jinmei Luo,[a] Peihui Yang*[a] and Jiye Cai[ab]

Received 23rd August 2014
Accepted 16th September 2014

DOI: 10.1039/c4an01532k

www.rsc.org/analyst

A highly sensitive and recyclable quartz crystal microbalance (QCM) biosensor was developed using chitosan (CS) and folic acid (FA), generating conjugates that are selectively recognized by MCF-7 cancer cell over-expressed folic acid receptors. The prepared CS–FA conjugate was characterized by UV-vis spectroscopy and Fourier transform infrared spectroscopy. Atomic force microscopy and scanning electron microscopy further presented the morphology of the CS–FA conjugate interface. The hydrophilicity of films was characterized by measuring the contact angle. The recognition of MCF-7 cancer cells was investigated *in situ* using QCM. Captured by FA, the concentration of the MCF-7 cell was determined on-line using a quartz crystal microbalance and a wide linear range of 4.5×10^2 to 1.01×10^5 cells per mL was obtained, with a detection limit of 430 cells per mL. The fluorescence microscope further confirmed the specificity and biocompatibility of the constructed biosensor. In addition, the regeneration of the QCM biosensor was studied by using lysozyme. This receptor-bound ligand based QCM biosensor also showed good selectivity, and repeatability in the cell mixture. For the first time, this simple, economical and label-free chitosan-based QCM sensing was demonstrated, and such design could provide a promising detection strategy for sensitive detection of cancer cell over-expressed folic acid receptors.

1. Introduction

Nowadays, breast cancer is the most common women's cancer worldwide. Development of early detection techniques for breast cancer is primarily important for improving survival rates.[1,2] Conventional diagnostic methods, including polymerase chain reaction (PCR)-based methods,[3,4] cytometric methods,[5] and cell-enrichment,[6] have been developed for cancer cell analysis. Although they have a high detection rate, many of these methods are expensive and time-consuming. They also require advanced instrumentation and enrichment of the target cells in the sample or expression of protein biomarkers or antibodies in the cells. Therefore, the developments of simple, time-saving, convenient and more economical methods for cancer cell detection are still needed.

The most recent efforts in cancer cell detection have focused on biosensors with good sensitivity and selectivity, as well as rapid and easy operation. Various biosensors using different transducers have been reported as effective in detecting and identifying cancer cells, including those based on electrochemical measurements,[7–12] fluorescence measurements,[13,14] single nanotube field effect transistor arrays[15] and microfluidic devices.[16] Although many of them have been applied at the laboratory research level, they are difficult to regenerate or suffer from time-consuming steps for labeling or off-line analysis. Hence, constructing a biosensor that avoids labor-intensive labeling steps and can be regenerated and allows real-time, on-line analysis is of great importance for simple and rapid cell analysis.

Alternatively, more attention has been paid to quartz crystal microbalance (QCM) as a sensor due to its rapid analysis speed, satisfactory sensitivity, simple instrumentation, and low cost.[17,18] QCM is a non-invasive, real-time and label-free technology that has been applied in many cell researches such as attachment, adhesion and spreading of cells on diverse kinds of coating layers.[19–21] The QCM technique can also detect the cellular responses to drugs[22] and exogenous stimulations,[23] nanoparticles,[24] or microparticles.[6] The advantages of QCM in these studies are that it can be used as a continuous monitoring device and can detect cumulative effects in a non-invasive way with high sensitivity. However, only a few references have reported the detection of cancer cells *via* QCM. Pan *et al.*[6] proposed a method for collection and detection of leukemia cells on a magnet-quartz crystal microbalance system using aptamer-conjugated magnetic beads, but this method suffers from time-consuming steps for collection of cells. Shan *et al.*[17]

[a]*Department of Chemistry, Jinan University, Guangzhou 510632, People's Republic of China. E-mail: typh@jnu.edu.cn; zhangshaolian1990@163.com; Fax: +86-20-85223569; Tel: +86-20-85223569*

[b]*State Key Laboratory of Quality Research in Chinese Medicines, Macau University of Science and Technology, Macau, China*

developed an aptamer-based QCM biosensor for detection of leukemia cells, but the artificial aptamer is expensive and difficult to regenerate after being immobilized on the QCM sensor surface. Nevertheless, QCM cytosensors are still in the development phase, the key is to develop a recyclable functionalized biosensor interface with good biocompatibility for selective recognition and capture of target cancer cells.

Thus, choosing interface materials was the critical step in the preparation of a recyclable functionalized biosensor. Chitosan (CS), an abundant natural biological macromolecule in the world, has attracted high consideration due to its non-toxicity, biocompatibility and biodegradability.[25] Much attention has been paid to CS-based biomedical materials and their applications in tissue engineering.[26,27] Until now, many chitosan-based QCM cytosensors have been reported to study cell adhesion,[28,29] however, few reports have focused on using chemically coupled functional chitosan in cancer cell detection field. Therefore, in order to make the sensor specific for cancer cells, the CS was functionalized with folic acid (FA). FA can specifically target folate receptors (FRs), which are the protein receptors on the surface of the cell membrane and usually over-expressed on some tumor cells.[30] Such design extends the application of chitosan in QCM biosensors, providing a promising approach for the development of QCM cytosensors.

In this study, we conjugated FA with water soluble low molecular weight chitosan for the fabrication of a bio-functional interface on gold substrates for the first time. Folic acid can specifically recognize folate receptors over-expressed on the MCF-7 cancer cell membrane and then capture the MCF-7 cancer cells, thus high selectivity for tumor cells can be obtained in comparison with normal cells in the fabricated chitosan-based QCM cytosensors. We demonstrate that the as-prepared cytosensor shows a sensitive response to MCF-7 cells with a detection limit of 430 cells per mL; above all, this prepared chitosan-based QCM biosensor shows good regeneration, reproducibility and stability, which offer a new avenue to chitosan applications in QCM cytosensing and other bioassays. In addition, the MCF-7 standard spiked blood sample was used to explore the potential of this method in practical applications. The method is simple, convenient and economical for breast cancer cell detection, and has the potential for other cancer cell detection as well.

2. Materials and methods

2.1. Reagents and materials

Human breast cancer cell lines MCF-7, human umbilical vein endothelial cells (HUVECs), oral epithelial cell lines H376 were obtained from the Institute of Physiology, Jinan University. RPMI 1640 medium, EGM-2 medium, Eagle's medium (DMEM)/Hams F12 nutrient, and fetal bovine serum (FBS) were purchased from Gibco Co. Chitosan (CS, deacetylation degree of 85% and molecular weight of 37.6 KDa) was purchased from Golden-shell Biochemical Co., Ltd. Folic acid (FA), 1-(3-dimethylaminopropyl)-3-ethylcarbodiimide hydrochloride (EDC), *N*-hydroxysuccinimide (NHS), bovine serum albumin (BSA) were obtained from Sigma-Aldrich. Phosphate-buffered saline (PBS) solution consisting of 136.7 mmol L^{-1} NaCl, 2.7 mmol L^{-1} KCl, 9.7 mmol L^{-1} Na_2HPO_4 and 1.5 mmol L^{-1} KH_2PO_4 was used. All other reagents are analytical reagents. Nanopure deionized and distilled water (18.2 MΩ) was used throughout all experiments.

2.2. Apparatus and characterizations

AT-cut 5 MHz quartz crystals (14 mm diameter) with a gold electrode (10 mm diameter) formed uniformly on one side were used. The resonant frequency of a quartz crystal was measured with a KSV QCM-Z500 quartz crystal microbalance system (KSV Instrument Ltd., Finland). The data recorded by QCM were analyzed by QcmZBrwse software. The ultraviolet-visible (UV-vis) absorption spectra were recorded with a UV-1901 UV-vis spectrophotometer (Beijing, China). Fourier transform infrared spectroscopy (FT-IR) analyses were performed on a Nicolet 6700 FT-IR spectrometer (Nicolet, USA). Water contact angle measurements were performed using a contact angle meter (CAM-PLUS; TANTEC company, German) at room temperature. 5 μL water droplet was used in the experiment by the sessile drop method, the reported values of the contact angle were the averages of five measurements at different positions of the same sample in this paper. The morphology of the films was characterized by scanning electron microscopy (SEM) (JEOL-JSM-6700F) and AutoProbe CP Research atomic force microscopy (AFM, Veeco, USA) in tapping mode. Fluorescent images were acquired on a Nikon inverted microscope (ECLIPSE TE-2000U, Nikon Corporation, Japan) equipped with a video camera (DS-U1, Nikon Corporation, Japan).

2.3. Synthesis of CS–FA

The conjugate of CS–FA was synthesized according to Mansouri's method.[31] Briefly, FA in anhydrous DMSO was prepared by stirring at room temperature until FA was well dissolved. Then, 0.4 M EDC and 0.1 M NHS were added and kept for 3 h at 4 °C. In this step, a certain amount of mixture solution of EDC and NHS was added to the above solution to activate the carboxyl group of FA and form an NHS ester. It was then added to a solution of 1% (w/v) chitosan (MW: 150 kDa) in acetate buffer (pH 4.7). The active NHS ester was replaced by the primary amines present in the chitosan, and the chitosan was thus immobilized through the amide bond. The resulting mixture was stirred at room temperature in the dark for 16 h. It was brought to pH 9.0 by drop wise addition of diluted aqueous NaOH and dialyzed first against phosphate buffer pH 7.4 for 3 days and then against water for 3 days.

2.4. Cell culture

The MCF-7 cell culture conditions followed the reported protocols.[32] Briefly, human breast cancer cell lines MCF-7 were grown in RPMI 1640 culture media supplemented with 100 U ml^{-1} streptomycin, 100 U ml^{-1} penicillin and 10% fetal bovine serum at 37 °C in a humidified atmosphere of 5% CO_2. Erythrocytes were separated from whole blood by centrifugation (3000 × *g*, 10 min) and then washed three times with PBS buffered solution.

Human umbilical vein endothelial cells (HUVECs) were cultured as described previously.[33] In brief, HUVECs were cultured in flasks at 37 °C in a CO_2 (5%) incubator. Once the cells reached 80% confluence, they were sub-cultured in 35 mm Petri dishes (Greiner) pre-coated with gelatin from fish skin (Sigma) and grown to confluence.

Oral epithelial cell lines H376 were cultured using the protocols reported in the literature.[34] Cells were cultured at 37 °C and 5% (v/v) CO_2 in Dulbecco's modified Eagle's medium (DMEM)/Hams F12 nutrient mix with 1 μg L^{-1} glucose supplemented with 10% (v/v) heat-inactivated foetal calf serum, 20 mM l-glutamine, 0.5 g mL^{-1} hydrocortisone (Sigma-Aldrich, UK) and 2500 IU mL^{-1} penicillin and streptomycin.

2.5. Fluorescent and MCF-7 cell image

ITO glass was chosen as a substrate in the fabrication of a biosensor. After successive sonication in ethanol, acetone and deionized water, ITO was rinsed with deionized water and dried at room temperature. Similar modification on ITO was carried out as that of QCM. Thus the prepared CS–FA/Au was immersed into 100 μL of 10.0 mg mL^{-1} BSA solution at 4 °C for 1 h to block active sites, carefully rinsed with PBS (pH = 7.4) and dried at room temperature. Then the modified ITO was immersed into the cell suspension at 4 °C for 2 h, washed thoroughly with PBS again, and finally dropped with 100 μL calcein-AM for 10 min. Images were taken by a Nikon inverted microscope. Excitations and filters were as follows: excitation filter 405 nm, LP 430 nm filter.

2.6. QCM measurements

All binding process was monitored on-line by using a KSV QCM-Z500 instrument at 25 °C with a flow rate of 200 μL min^{-1}. Prior to modification, crystal chips (5 MHz, AT-cut) (QSX 301, Q-Sense AB, Sweden) used were immersed in a boiling solution (30% H_2O_2, 28% ammonia, and deionized water in a volume ratio of 1 : 1 : 5) for 5 min. The washed chips were then rinsed thoroughly with deionized water, dried by nitrogen gas prior to use.

The conjugate of CS–FA prepared above was spin-coated to the cleaned QCM gold electrode, dried in a silica gel desiccator, and then the quartz crystal was fixed to the QCM chamber. The obtained modified chip was thoroughly rinsed with PBS buffer and then used as the sensor surface for MCF-7 cell determination. The MCF-7 cell sample was injected into the QCM chamber for direct analysis, followed by rinsing with PBS buffer solution to remove non-bound cells. Scheme 1 shows the schematic diagram of preparation of the QCM biosensor.

2.7. Data analysis

The frequency and dissipation changes were monitored by instruments of QCM, data analysis was performed using QcmZBrwse software from Q-Sense.

3. Results and discussion

3.1. Characterization of CS–FA

The functionalized CS (CS–FA), CS and glass slide were characterized using AFM and SEM and are shown in Fig. 1. Fig. 1A shows the AFM images obtained for CS–FA, CS and glass slide, respectively. It was found that the roughness of the CS–FA film is higher than the CS, suggesting that the CS–FA interface is getting rougher and the surface area is increasing so that more MCF-7 cells can be recognized. Fig. 1B also shows the images of an additional characterization of the film surface by SEM. The image of CS–FA in Fig. 1B reveals the cross-linked structure of CS–FA, which also confirmed the AFM image. The results for the control (glass slide) are also shown for the sake of comparison. The above images revealed that FA was successfully coupled to CS.

Fig. 2A shows the UV-vis absorption spectra of CS, FA and FA–CS, respectively. In the case of CS, the extremely weak absorption peak corresponding to the n → π* transition shifted to 300 nm. For FA, two absorption peaks were observed, one was at 280 nm, corresponding to the π → π* transition of the C=C bond, and the other was at 360 nm, corresponding to the n → π* transition of the C=O bond. Whereas FA–CS has a

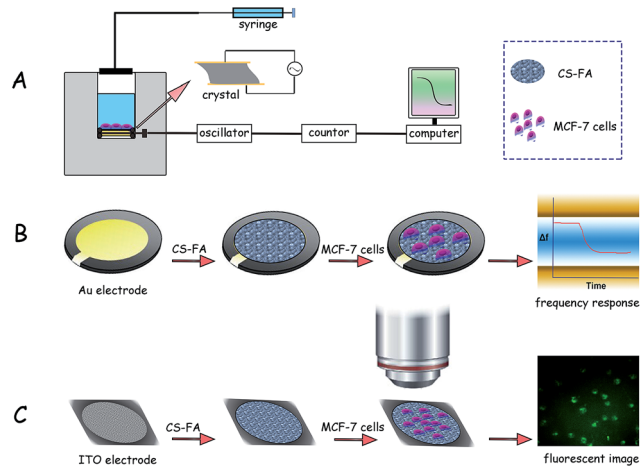

Scheme 1 (A) Schematic diagram of the experimental set-up. (B) The schematic representation of the label-free QCM biosensor for on-line detection of MCF-7 cancer cells. (C) Fluorescent image of the biosensor after capturing MCF-7 cancer cells.

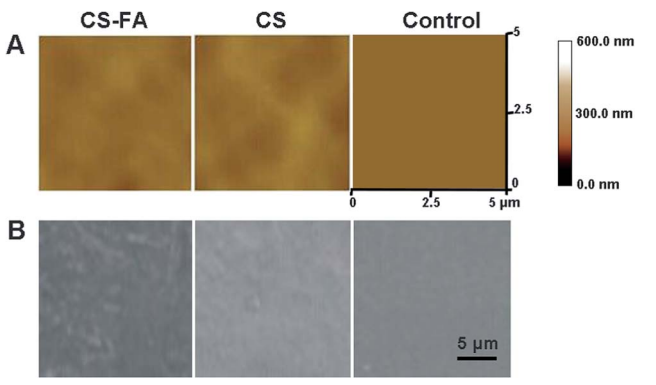

Fig. 1 Representative AFM (A) and SEM (B) images of CS–FA and CS films. The images of the control (glass slide) are also shown for the sake of comparison.

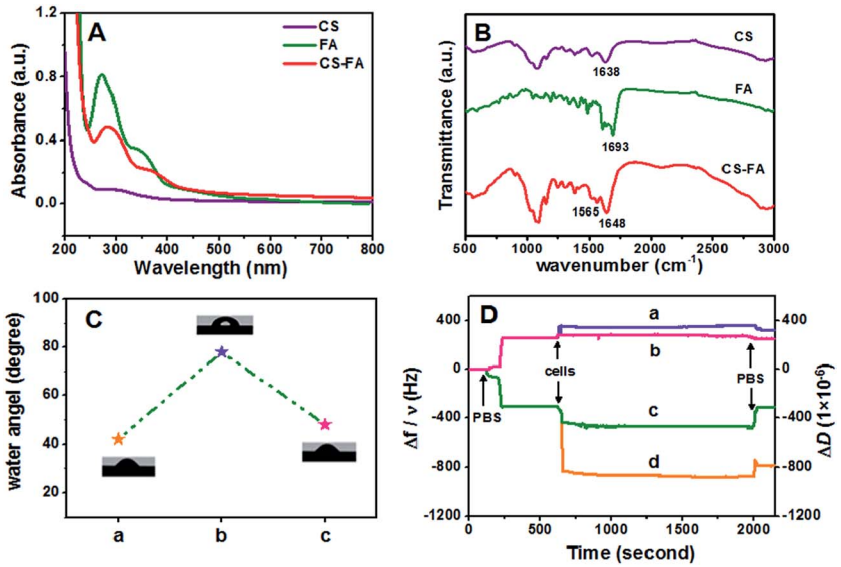

Fig. 2 (A) UV-vis spectra and (B) FT-IR spectra of CS, FA and CS–FA. (C) Contact angle of the bare Au electrode (a), CS/Au (b) and CS–FA/Au (c). (D) Time-dependent frequency (c and d) and dissipation (a and b) responses of the QCM biosensor. The profile (650 s < t < 2000 s) represents the recognition of 1.0 × 10^3 cells per mL of MCF-7 cancer cells (a and d) and 1.0 × 10^3 cells per mL of endothelial cells (b and c). Control curves show the responses resulted from PBS buffer solution.

strong absorption peak at 280 nm and a weak absorption peak at 360 nm, which confirmed the successful conjugation of FA with CS.[35,36]

The FT-IR was further performed for the confirmation of successful coupling of FA to CS. Fig. 2B shows the FT-IR spectra of CS, FA and FA–CS composites respectively. In Fig. 2B, all specimens show the characteristic peak at 1420 and ~3400 cm^{-1}, which was attributed to the flexural vibration of CH_2 and stretching vibration of N–H, respectively.[37] The FT-IR spectra of CS show two bands located at around 1638 cm^{-1} and 1596 cm^{-1} which could be assigned to amino I and amino II functional groups of the native CS, respectively.[27] The bands observed at 1693 cm^{-1} and ~1608 cm^{-1} of FA correspond to the C=O stretching vibration and the N–H deformation.[38] CS–FA exhibits more distinctive bands associated with FA conjugation, amide I and amide II at 1648 and 1565 cm^{-1}, and –OH stretching and N–H stretching vibration centred at ~3360 cm^{-1}. The C=O stretching band of residual COOH of conjugated FA was not noted, but it may overlay with amide I, as occurred in native FA.[35,39]

The surface nature of materials, such as the surface charge, hydrophilicity and wettability, is important for cell attachment or proliferation.[40] The hydrophilicity of films was characterized by measuring the contact angle. As shown in Fig. 2C, the corresponding contact angles for bare Au, CS and CS–FA were 42.0°, 78.2° and 48.4°, respectively. Compared to CS, CS–FA had better hydrophilicity which was in favor of enhancing the loading of cells and retaining their bioactivity. The CS–FA film showed the lower contact angle, indicating the best hydrophilicity, attributed to the carboxyl and hydroxyl groups in FA and CS. The results showed that the film could provide a biocompatible surface and promote cell adhesion and growth.

The recognition of 1 × 10^5 cells per mL of MCF-7 cancer cells and HUVEC non-cancerous cells was investigated in real-time using the QCM technique (Fig. 2D). For graphical simplification, the results in this figure present frequency (Δf) shift and energy dissipation (ΔD) changes as a function of time for the 3rd harmonic. As shown in Fig. 2D, $\Delta f/v$ values of MCF-7 cells (curve d) captured by the biosensor were 3 times greater than those of HUVEC signals (curve c). This is due to the over-expression of FR molecules on the MCF-7 cell surface and then specific recognition by the biosensor, thus, the binding of cells to the FA molecule-functionalized biosensor further added the mass on the oscillating quartz crystal sensor, leading to a remarkable frequency decrease. Regarding energy dissipation factor, ΔD characterizes the viscoelasticity of the attached layer formed on top of the sensing surface. ΔD is defined as the ratio of the dissipated energy and the energy elastically stored per cycle.[41] As can be observed from curve a in Fig. 2D, the injection of MCF-7 cells causes a dissipation increase due to the viscoelastic nature of the adsorbed cell layer, like the typical of polymeric systems. Interestingly, none or very low ΔD signals was obtained by the biosensor in the non-cancerous cells (curve b). This might be due to the less expression of the FR molecule on the non-cancerous cell surface and the FA-functionalized sensor surface trapped less HUVECs, leading to a low dissipation shift. When rinsing with PBS buffer solution after recognition, an increase in $\Delta f/v$ and a slight decrease in ΔD were observed due to the rinsing of non-specifically adsorbed molecules. According to the remarkably different QCM signals of cancer and non-cancerous cells, it could be indicated that the amount of folic acid receptors expressed on cancer cell surfaces was different from non-cancerous cells.

3.2. Optimization of synthesis of CS–FA

In this work, the QCM frequency signal intensity of the MCF-7 cells captured by the CS–FA interface was determined by the amount of FA in the conjugate. Thus, optimization of the reaction conditions is necessary to plot the calibration curve, and as shown in Fig. 3A, the degree of increasing absorption intensity was linearly related to the concentration of FA. They all have an excitation band at approximately 280 nm, similar to the conjugate band. The influence of the FA concentration on the maximum UV-vis absorption intensity was investigated by using different mass ratios of CS to FA. Fig. 3B shows that the absorption intensity increased with an increased FA ratio and tended to be constant beyond 1 : 4 ($M_{CS} : M_{FA}$). Over the ratio of 1 : 4, the absorption intensity did not change significantly due to the saturation effect. The error bars represent the standard deviation (S.D.) of three measurements. Hence, the optimal mass ratio of CS to FA was 1 : 4.

3.3. Analytical performance of the QCM biosensor

To evaluate the sensitivity and quantitative range of the proposed assay strategy, the novel assay format was employed to detect different concentrations of MCF-7 cells. It can be seen (Fig. 4) that the QCM frequency responses for the 7th harmonic increase accordingly as the concentration of MCF-7 is varied from 450 cells per mL to 1.01×10^5 cells per mL with a detection limit of 430 cells per mL ($S/N = 3$). The linear regression equation is $-\Delta f = 69.392 \log c - 168.577$ (where Δf is the QCM frequency intensity and c stands for the concentration of MCF-7 cells), and the correlation coefficient is $R^2 = 0.9984$. The results demonstrated that the proposed method could be used to detect the MCF-7 concentration quantitatively. Compared to other methods based on the QCM technique,[6,17] this proposed QCM cytosensor had a relatively wider linear range and lower detection limit.

3.4. Selectivity and specificity of the biosensor

In order to explore the selectivity of the present biosensor, contrast experiments were performed (Fig. 5). Erythrocytes, endothelial cells (HUVECs) and oral epithelial cell lines H376 were used as interfering substances to evaluate the selectivity and specificity of the proposed cytosensor. As shown in Fig. 5, the adsorptions of erythrocytes, HUVECs and H376 on CS–FA conjugates are all negligible with cell concentrations even up to 1.0×10^4 cells per mL. By contrast, the binding of CS–FA with 1.0×10^3 cells per mL of MCF-7 cells resulted in much larger frequency shifts. Moreover, a significant frequency shift was observed in the mixture of 1.0×10^3 cells per mL of erythrocytes, endothelial cells, oral epithelial cells and MCF-7 cells, respectively. These results demonstrate that the CS–FA modified QCM biosensor is highly specific for MCF-7 cells.

Fluorescence microscopy was used to characterize the CS–FA cytosensor for the recognition of MCF-7 cells because they could express high levels of FR.[42] Low-toxic calcein-AM was chosen to carry out the staining experiment for the determination of cell viability since its fluorescence intensity was proportional to the amount of live cells.[35,43] As shown in Fig. 6A, a homogeneous fluorescence was observed when the electrode was not exposed to cells. After the CS–FA/ITO was incubated into the solution with MCF-10 cells for 2 h, a weak fluorescence could be observed (Fig. 6B), which means that few viable cells were adhered on the CS–FA film. However, a strong fluorescence was

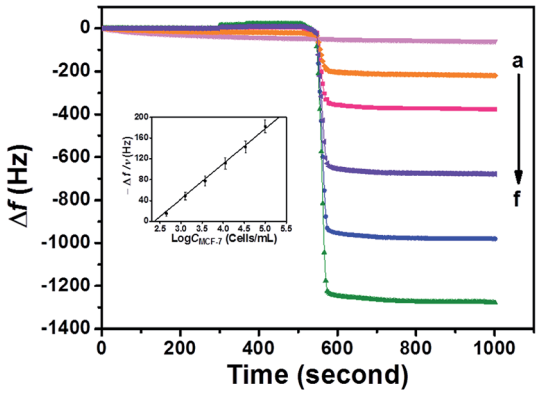

Fig. 4 Real-time frequency responses of the CS–FA modified QCM biosensor for the MCF-7 cell. (a) 4.5×10^2, (b) 1.25×10^3, (c) 3.75×10^3, (d) 4.05×10^4, (e) 4.53×10^4, (f) 1.01×10^5 cells per mL, respectively. Insets: the linear relationships between the frequency shifts and the logarithms of MCF-7 cell concentrations. The error bars represent the standard deviation (S.D.) of three measurements.

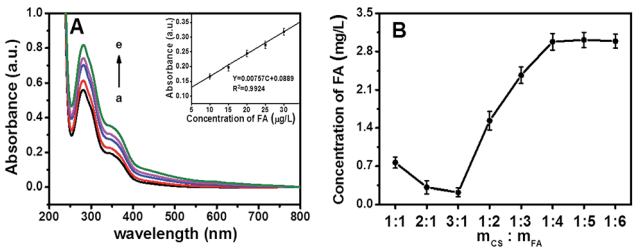

Fig. 3 (A) UV-vis spectra of FA solutions with different concentrations: (a) 10, (b) 15, (c) 20, (d) 25, (e) 30 μg L^{-1}, respectively. Inset: calibration plot of concentration of FA against absorbance intensity. (B) Determination of the concentration of FA in different conjugates of CS–FA. The error bars represent the standard deviation (S.D.) of three measurements.

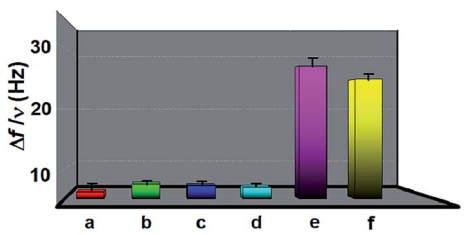

Fig. 5 Selectivity of the CS–FA modified QCM biosensor, (a) blank, (b) with 1.0×10^4 cells per mL of erythrocytes, (c) with 1.0×10^4 cells per mL of endothelial cells, (d) with 1.0×10^4 cells per mL of oral epithelial cells, (e) with 1.0×10^3 cells per mL of MCF-7 cells, (f) with the mixture of 1.0×10^4 cells per mL of erythrocytes, endothelial cells, oral epithelial cells and MCF-7 cells, respectively.

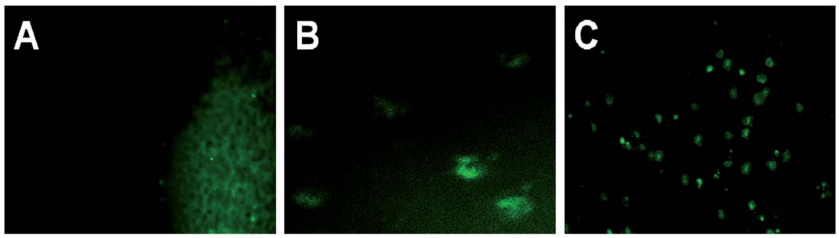

Fig. 6 Fluorescent images of the cells stained by calcein-AM after being captured for 2 h by the different interfaces: (A) the CS interface, (B) endothelial cells and (C) MCF-7 cells on the CS–FA interface.

observed after incubation into MCF-7 cells for 2 h (Fig. 6C), the attached round cells almost adhered and spreaded to irregular shapes on the surface of the film, indicating a good viability. Thus the CS–FA cytosensor did not show cytotoxicity and was suitable for the immobilization of cells with good biocompatibility and specificity.

3.5. Regeneration, reproducibility and stability of the cytosensor

The QCM-D chip after the recognition of MCF-7 cancer cells was regenerated by rinsing the surface firstly with 0.2 M lysozyme at pH 6 for 2 h, this resulted in a complete chitosan degradation into *N*-acetyl glucosamine, then lysozyme and *N*-acetyl glucosamine were then removed from the chip surface by the treatment with PBS (pH 7.4). After modifying the gold electrode and exposing to MCF-7 cells, the QCM biosensor could again capture cells. As shown in Fig. 7, after 5 cycles, the Δf values still remained 83%. The results from five cycles indicate that the chitosan-based QCM biosensor interface is biodegradable and the sensing surface is reusable. The regeneration method is superior to other methods,[44] which is due to the favorable biological properties of chitosan such as biodegradability, biocompatibility, low toxicity, as well as reasonable cost. The reproducibility of the QCM biosensor was estimated by determining the cell level with three cytosensors of different batches under the same experiment conditions. The relative standard deviation (RSD) of the inter-assay was 7.28% at the cell concentration of 1.0×10^4 cells per mL, indicating acceptable precision and fabrication reproducibility. The cytosensor retained its QCM response after 2 weeks at 4 °C, without obvious decline. This indicated that the CS–FA modified gold electrode was efficient to hold its stability and bioactivity as well.

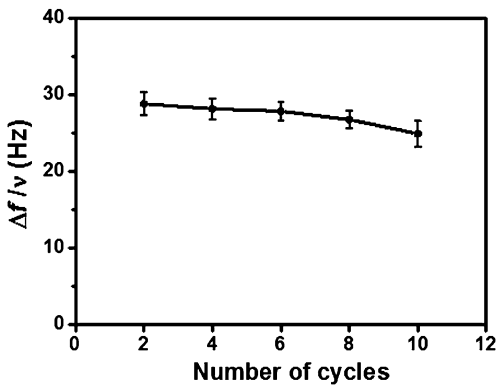

Fig. 7 Frequency response of the chitosan-based QCM biosensor to 1.0×10^3 cells per mL of MCF-7 cells after regeneration cycles. The error bars represent the standard deviation (S.D.) of three measurements.

3.6. Analysis of the standard spiked blood sample

To verify the preliminary validity of the present biosensor in the complex matrix, this CS–FA modified QCM system was applied for the determination of MCF-7 in the standard spiked blood sample. For the dilution fold of 5, 10 and 20, the obtained recoveries for MCF-7 (1×10^4 cells per mL) in spiked blood were 119%, 115% and 108% with corresponding relative standard deviations ($n = 3$) of 11%, 8% and 6%, respectively. This result suggests that the CS–FA modified QCM biosensor exhibits satisfactory analytical ability towards cancer cell over-expressed FRs in the blood sample.

4. Conclusions

An effective strategy for the preparation of CS–FA with high biocompatibility and specificity was developed, and it could be used to fabricate a QCM biosensor for label-free MCF-7 breast cancer cell detection. The cytosensor when functionalized with FA as a target anchorage to capture MCF-7 cells specifically exhibited desirable performance for cancer cell detection. Therefore, we anticipate that this research will further facilitate the application of functionalized chitosan for biosensing applications and provide a convenient platform for clinical diagnoses in the future.

Acknowledgements

This work was supported by grants from the National Natural Science Foundation of China (no. 21375048) and the Major State Basic Research Development Program of China (973 Program) (no. 2010CB833603).

References

1 Y.-F. Chang, S.-H. Hung, Y.-J. Lee, R.-C. Chen, L.-C. Su, C.-S. Lai and C. Chou, *Anal. Chem.*, 2011, **83**, 5324–5328.

2 A. Jemal, F. Bray, M. M. Center, J. Ferlay, E. Ward and D. Forman, *Ca-Cancer J. Clin.*, 2011, **61**, 69–90.
3 N. Berois, M. Varangot, C. Sonora, L. Zarantonelli, C. Pressa, R. Lavina, J. L. Rodriguez, F. Delgado, N. Porchet, J. P. Aubert and E. Osinaga, *Int. J. Cancer*, 2003, **103**, 550–555.
4 H. Yin, Y. Zhou, C. Chen, L. Zhu and S. Ai, *Analyst*, 2012, **137**, 1389–1395.
5 L. Dumartin, H. J. Whiteman, M. E. Weeks, D. Hariharan, B. Dmitrovic, C. A. Iacobuzio-Donahue, T. A. Brentnall, M. P. Bronner, R. M. Feakins, J. F. Timms, C. Brennan, N. R. Lemoine and T. Crnogorac-Jurcevic, *Cancer Res.*, 2011, **71**, 7091–7102.
6 Y. Pan, M. Guo, Z. Nie, Y. Huang, C. Pan, K. Zeng, Y. Zhang and S. Yao, *Biosens. Bioelectron.*, 2010, **25**, 1609–1614.
7 M. Yan, G. Q. Sun, F. Liu, J. J. Lu, J. H. Yu and X. R. Song, *Anal. Chim. Acta*, 2013, **798**, 33–39.
8 C. Hu, D.-P. Yang, Z. Wang, L. Yu, J. Zhang and N. Jia, *Anal. Chem.*, 2013, **85**, 5200–5206.
9 C. Hu, D.-P. Yang, Z. Wang, P. Huang, X. Wang, D. Chen, D. Cui, M. Yang and N. Jia, *Biosens. Bioelectron.*, 2013, **41**, 656–662.
10 C. Hu, D.-P. Yang, K. Xu, H. Cao, B. Wu, D. Cui and N. Jia, *Anal. Chem.*, 2012, **84**, 10324–10331.
11 C. Hu, D.-P. Yang, F. Zhu, F. Jiang, S. Shen and J. Zhang, *ACS Appl. Mater. Interfaces*, 2014, **6**, 4170–4178.
12 S. Zhang, L. Zhang, X. Zhang, P. Yang and J. Cai, *Analyst*, 2014, **139**, 3629–3635.
13 J. Camps, I. Ponsa, M. Ribas, E. Prat, J. Egozcue, M. A. Peinado and R. Miro, *FASEB J.*, 2005, **19**, 828–847.
14 Y. Fu, D. Lu, B. Lin, Q. Sun, K. Liu, L. Xu, S. Zhang, C. Hu, C. Wang, Z. Xu and W. Zhang, *Analyst*, 2013, **138**, 7016–7022.
15 Q. Liu, T. Zhang, L. Yu, N. Jia and D.-P. Yang, *Analyst*, 2013, **138**, 5559–5562.
16 A. Weltin, K. Slotwinski, J. Kieninger, I. Moser, G. Jobst, M. Wego, R. Ehret and G. A. Urban, *Lab Chip*, 2014, **14**, 138–146.
17 W. Shan, Y. Pan, H. Fang, M. Guo, Z. Nie, Y. Huang and S. Yao, *Talanta*, 2014, **126**, 130–135.
18 R. Hao, D. Wang, X. e. Zhang, G. Zuo, H. Wei, R. Yang, Z. Zhang, Z. Cheng, Y. Guo and Z. Cui, *Biosens. Bioelectron.*, 2009, **24**, 1330–1335.
19 M. Guo, J. Chen, Y. Zhang, K. Chen, C. Pan and S. Yao, *Biosens. Bioelectron.*, 2008, **23**, 865–871.
20 B. Thierry and H. J. Griesser, *J. Mater. Chem.*, 2012, **22**, 8810–8819.
21 T. W. Chung, Y. C. Tyan, R. H. Lee and C. W. Ho, *J. Mater. Sci.: Mater. Med.*, 2012, **23**, 3067–3073.
22 K. A. Marx, T. Zhou, A. Montrone, D. McIntosh and S. J. Braunhut, *Anal. Biochem.*, 2007, **361**, 77–92.
23 M. Tarantola, E. Sunnick, D. Schneider, A.-K. Marel, A. Kunze and A. Janshoff, *Chem. Res. Toxicol.*, 2011, **24**, 1494–1506.
24 G. Garai-Ibabe, R. Grinyte, E. I. Golub, A. Canaan, M. L. de la Chapelle, R. S. Marks and V. Pavlov, *Biosens. Bioelectron.*, 2011, **30**, 272–275.
25 M. Garcia-Fuentes and M. J. Alonso, *J. Controlled Release*, 2012, **161**, 496–504.
26 R. F. F. de Araujo, C. R. Martinez, K. P. D. Luna, R. M. C. Souza, D. Bruneska, R. F. Dutra and J. L. de Lima, *Appl. Surf. Sci.*, 2013, **274**, 33–38.
27 V. M. Esquerdo, T. R. S. Cadaval Jr, G. L. Dotto and L. A. A. Pinto, *J. Colloid Interface Sci.*, 2014, **424**, 7–15.
28 L. Zhao, Y. Hu, D. Xu and K. Cai, *Colloids Surf., B*, 2014, **119**, 115–125.
29 A. I. Neto, A. C. Cibrao, C. R. Correia, R. R. Carvalho, G. M. Luz, G. G. Ferrer, G. Botelho, C. Picart, N. M. Alves and J. F. Mano, *Small*, 2014, **10**, 2459–2469.
30 R. Li, C. Wang, Y. Hu, O. Zheng, L. Guo, Z. Lin, B. Qiu and G. Chen, *Biosens. Bioelectron.*, 2014, **58**, 226–231.
31 S. Mansouri, Y. Cuie, F. Winnik, Q. Shi, P. Lavigne, M. Benderdour, E. Beaumont and J. C. Fernandes, *Biomaterials*, 2006, **27**, 2060–2065.
32 L. Zhang, F. Yang, J.-Y. Cai, P.-H. Yang and Z.-H. Liang, *Biosens. Bioelectron.*, 2014, **56**, 271–277.
33 L. Tan, P. Lin, B. Pezeshkian, A. Rehman, G. Madlambayan and X. Zeng, *Biosens. Bioelectron.*, 2014, **56**, 151–158.
34 J. Elsom, M. I. Lethem, G. D. Rees and A. C. Hunter, *Biosens. Bioelectron.*, 2008, **23**, 1259–1265.
35 G. Yang, J. Cao, L. Li, R. K. Rana and J.-J. Zhu, *Carbon*, 2013, **51**, 124–133.
36 P. M. S. D. Cal, R. F. M. Frade, V. Chudasama, C. Cordeiro, S. Caddick and P. M. P. Gois, *Chem. Commun.*, 2014, **50**, 5261–5263.
37 B. Ma, A. Qin, X. Li, X. Zhao and C. He, *Int. J. Biol. Macromol.*, 2014, **64**, 341–346.
38 Y. Hu, B. Ma, Y. Zhang and M. Wang, *Biomed. Microdevices*, 2014, **16**, 487–497.
39 A. K. Agrawal, H. Harde, K. Thanki and S. Jain, *Biomacromolecules*, 2014, **15**, 350–360.
40 Y. Song, Y. Chen, L. Feng, J. Ren and X. Qu, *Chem. Commun.*, 2011, **47**, 4436–4438.
41 V. Heitmann and J. Wegener, *Anal. Chem.*, 2007, **79**, 3392–3400.
42 Y. Mi, Y. Liu and S.-S. Feng, *Biomaterials*, 2011, **32**, 4058–4066.
43 P. Grieshaber, W. A. Lagrèze, C. Noack, D. Boehringer and J. Biermann, *J. Neurosci. Methods*, 2010, **192**, 233–239.
44 Q. Chen, W. Tang, D. Wang, X. Wu, N. Li and F. Liu, *Biosens. Bioelectron.*, 2010, **26**, 575–579.